Measurement of the branching fractions of the rare decays $B^0 \to D_s^{(*)+}\pi^-$, $B^0 \to D_s^{(*)+}\rho^-$, and $B^0 \to D_s^{(*)-}K^{(*)+}$

B. Aubert,[1] M. Bona,[1] Y. Karyotakis,[1] J. P. Lees,[1] V. Poireau,[1] E. Prencipe,[1] X. Prudent,[1] V. Tisserand,[1] J. Garra Tico,[2] E. Grauges,[2] L. Lopez,[3] A. Palano,[3] M. Pappagallo,[3] G. Eigen,[4] B. Stugu,[4] L. Sun,[4] G. S. Abrams,[5] M. Battaglia,[5] D. N. Brown,[5] J. Button-Shafer,[5] R. N. Cahn,[5] R. G. Jacobsen,[5] J. A. Kadyk,[5] L. T. Kerth,[5] Yu. G. Kolomensky,[5] G. Kukartsev,[5] G. Lynch,[5] I. L. Osipenkov,[5] M. T. Ronan,[5,*] A. Suzuki,[5] K. Tackmann,[5] T. Tanabe,[5] W. A. Wenzel,[5] C. M. Hawkes,[6] N. Soni,[6] A. T. Watson,[6] H. Koch,[7] T. Schroeder,[7] D. Walker,[8] D. J. Asgeirsson,[9] T. Cuhadar-Donszelmann,[9] B. G. Fulsom,[9] C. Hearty,[9] T. S. Mattison,[9] J. A. McKenna,[9] M. Barrett,[10] A. Khan,[10] M. Saleem,[10] L. Teodorescu,[10] V. E. Blinov,[11] A. D. Bukin,[11] A. R. Buzykaev,[11] V. P. Druzhinin,[11] V. B. Golubev,[11] A. P. Onuchin,[11] S. I. Serednyakov,[11] Yu. I. Skovpen,[11] E. P. Solodov,[11] K. Yu. Todyshev,[11] M. Bondioli,[12] S. Curry,[12] I. Eschrich,[12] D. Kirkby,[12] A. J. Lankford,[12] P. Lund,[12] M. Mandelkern,[12] E. C. Martin,[12] D. P. Stoker,[12] S. Abachi,[13] C. Buchanan,[13] J. W. Gary,[14] F. Liu,[14] O. Long,[14] B. C. Shen,[14,*] G. M. Vitug,[14] Z. Yasin,[14] L. Zhang,[14] V. Sharma,[15] C. Campagnari,[16] T. M. Hong,[16] D. Kovalskyi,[16] M. A. Mazur,[16] J. D. Richman,[16] T. W. Beck,[17] A. M. Eisner,[17] C. J. Flacco,[17] C. A. Heusch,[17] J. Kroseberg,[17] W. S. Lockman,[17] T. Schalk,[17] B. A. Schumm,[17] A. Seiden,[17] L. Wang,[17] M. G. Wilson,[17] L. O. Winstrom,[17] C. H. Cheng,[18] D. A. Doll,[18] B. Echenard,[18] F. Fang,[18] D. G. Hitlin,[18] I. Narsky,[18] T. Piatenko,[18] F. C. Porter,[18] R. Andreassen,[19] G. Mancinelli,[19] B. T. Meadows,[19] K. Mishra,[19] M. D. Sokoloff,[19] F. Blanc,[20] P. C. Bloom,[20] W. T. Ford,[20] A. Gaz,[20] J. F. Hirschauer,[20] A. Kreisel,[20] M. Nagel,[20] U. Nauenberg,[20] A. Olivas,[20] J. G. Smith,[20] K. A. Ulmer,[20] S. R. Wagner,[20] R. Ayad,[21,+] A. M. Gabareen,[21] A. Soffer,[21,‡] W. H. Toki,[21] R. J. Wilson,[21] D. D. Altenburg,[22] E. Feltresi,[22] A. Hauke,[22] H. Jasper,[22] M. Karbach,[22] J. Merkel,[22] A. Petzold,[22] B. Spaan,[22] K. Wacker,[22] V. Klose,[23] M. J. Kobel,[23] H. M. Lacker,[23] W. F. Mader,[23] R. Nogowski,[23] K. R. Schubert,[23] R. Schwierz,[23] J. E. Sundermann,[23] A. Volk,[23] D. Bernard,[24] G. R. Bonneaud,[24] E. Latour,[24] Ch. Thiebaux,[24] M. Verderi,[24] P. J. Clark,[25] W. Gradl,[25] S. Playfer,[25] J. E. Watson,[25] M. Andreotti,[26] D. Bettoni,[26] C. Bozzi,[26] R. Calabrese,[26] A. Cecchi,[26] G. Cibinetto,[26] P. Franchini,[26] E. Luppi,[26] M. Negrini,[26] A. Petrella,[26] L. Piemontese,[26] V. Santoro,[26] F. Anulli,[27] R. Baldini-Ferroli,[27] A. Calcaterra,[27] R. de Sangro,[27] G. Finocchiaro,[27] S. Pacetti,[27] P. Patteri,[27] I. M. Peruzzi,[27,§] M. Piccolo,[27] M. Rama,[27] A. Zallo,[27] A. Buzzo,[28] R. Contri,[28] M. Lo Vetere,[28] M. M. Macri,[28] M. R. Monge,[28] S. Passaggio,[28] C. Patrignani,[28] E. Robutti,[28] A. Santroni,[28] S. Tosi,[28] K. S. Chaisanguanthum,[29] M. Morii,[29] R. S. Dubitzky,[30] J. Marks,[30] S. Schenk,[30] U. Uwer,[30] D. J. Bard,[31] P. D. Dauncey,[31] J. A. Nash,[31] W. Panduro Vazquez,[31] M. Tibbetts,[31] P. K. Behera,[32] X. Chai,[32] M. J. Charles,[32] U. Mallik,[32] J. Cochran,[33] H. B. Crawley,[33] L. Dong,[33] W. T. Meyer,[33] S. Prell,[33] E. I. Rosenberg,[33] A. E. Rubin,[33] Y. Y. Gao,[34] A. V. Gritsan,[34] Z. J. Guo,[34] C. K. Lae,[34] A. G. Denig,[35] M. Fritsch,[35] G. Schott,[35] N. Arnaud,[36] J. Béquilleux,[36] A. D'Orazio,[36] M. Davier,[36] J. Firmino da Costa,[36] G. Grosdidier,[36] A. Höcker,[36] V. Lepeltier,[36] F. Le Diberder,[36] A. M. Lutz,[36] S. Pruvot,[36] P. Roudeau,[36] M. H. Schune,[36] J. Serrano,[36] V. Sordini,[36] A. Stocchi,[36] W. F. Wang,[36] G. Wormser,[36] D. J. Lange,[37] D. M. Wright,[37] I. Bingham,[38] J. P. Burke,[38] C. A. Chavez,[38] J. R. Fry,[38] E. Gabathuler,[38] R. Gamet,[38] D. E. Hutchcroft,[38] D. J. Payne,[38] C. Touramanis,[38] A. J. Bevan,[39] K. A. George,[39] F. Di Lodovico,[39] R. Sacco,[39] M. Sigamani,[39] G. Cowan,[40] H. U. Flaecher,[40] D. A. Hopkins,[40] S. Paramesvaran,[40] F. Salvatore,[40] A. C. Wren,[40] D. N. Brown,[41] C. L. Davis,[41] K. E. Alwyn,[42] N. R. Barlow,[42] R. J. Barlow,[42] Y. M. Chia,[42] C. L. Edgar,[42] G. D. Lafferty,[42] T. J. West,[42] J. I. Yi,[42] J. Anderson,[43] C. Chen,[43] A. Jawahery,[43] D. A. Roberts,[43] G. Simi,[43] J. M. Tuggle,[43] C. Dallapiccola,[44] S. S. Hertzbach,[44] X. Li,[44] E. Salvati,[44] S. Saremi,[44] R. Cowan,[45] D. Dujmic,[45] P. H. Fisher,[45] K. Koeneke,[45] G. Sciolla,[45] M. Spitznagel,[45] F. Taylor,[45] R. K. Yamamoto,[45] M. Zhao,[45] S. E. Mclachlin,[46,*] P. M. Patel,[46] S. H. Robertson,[46] A. Lazzaro,[47] V. Lombardo,[47] F. Palombo,[47] J. M. Bauer,[48] L. Cremaldi,[48] V. Eschenburg,[48] R. Godang,[48] R. Kroeger,[48] D. A. Sanders,[48] D. J. Summers,[48] H. W. Zhao,[48] S. Brunet,[49] D. Côté,[49] M. Simard,[49] P. Taras,[49] F. B. Viaud,[49] H. Nicholson,[50] G. De Nardo,[51] L. Lista,[51] D. Monorchio,[51] C. Sciacca,[51] M. A. Baak,[52] G. Raven,[52] H. L. Snoek,[52] C. P. Jessop,[53] K. J. Knoepfel,[53] J. M. LoSecco,[53] G. Benelli,[54] L. A. Corwin,[54] K. Honscheid,[54] H. Kagan,[54] R. Kass,[54] J. P. Morris,[54] A. M. Rahimi,[54] J. J. Regensburger,[54] S. J. Sekula,[54] Q. K. Wong,[54] N. L. Blount,[55] J. Brau,[55] R. Frey,[55] O. Igonkina,[55] J. A. Kolb,[55] M. Lu,[55] R. Rahmat,[55] N. B. Sinev,[55] D. Strom,[55] J. Strube,[55] E. Torrence,[55] G. Castelli,[56] N. Gagliardi,[56] M. Margoni,[56] M. Morandin,[56] M. Posocco,[56] M. Rotondo,[56] F. Simonetto,[56] R. Stroili,[56] C. Voci,[56] P. del Amo Sanchez,[57] E. Ben-Haim,[57] H. Briand,[57] G. Calderini,[57] J. Chauveau,[57] P. David,[57] L. Del Buono,[57] O. Hamon,[57] Ph. Leruste,[57] J. Ocariz,[57] A. Perez,[57] J. Prendki,[57] L. Gladney,[58] M. Biasini,[59] R. Covarelli,[59] E. Manoni,[59] C. Angelini,[60] G. Batignani,[60] S. Bettarini,[60] M. Carpinelli,[60,‖] A. Cervelli,[60] F. Forti,[60] M. A. Giorgi,[60] A. Lusiani,[60] G. Marchiori,[60] M. Morganti,[60] N. Neri,[60] E. Paoloni,[60] G. Rizzo,[60] J. J. Walsh,[60] J. Biesiada,[61] D. Lopes Pegna,[61] C. Lu,[61] J. Olsen,[61]

A. J. S. Smith,[61] A. V. Telnov,[61] E. Baracchini,[62] G. Cavoto,[62] D. del Re,[62] E. Di Marco,[62] R. Faccini,[62] F. Ferrarotto,[62] F. Ferroni,[62] M. Gaspero,[62] P. D. Jackson,[62] L. Li Gioi,[62] M. A. Mazzoni,[62] S. Morganti,[62] G. Piredda,[62] F. Polci,[62] F. Renga,[62] C. Voena,[62] M. Ebert,[63] T. Hartmann,[63] H. Schröder,[63] R. Waldi,[63] T. Adye,[64] B. Franek,[64] E. O. Olaiya,[64] W. Roethel,[64] F. F. Wilson,[64] S. Emery,[65] M. Escalier,[65] L. Esteve,[65] A. Gaidot,[65] S. F. Ganzhur,[65] G. Hamel de Monchenault,[65] W. Kozanecki,[65] G. Vasseur,[65] Ch. Yèche,[65] M. Zito,[65] X. R. Chen,[66] H. Liu,[66] W. Park,[66] M. V. Purohit,[66] R. M. White,[66] J. R. Wilson,[66] M. T. Allen,[67] D. Aston,[67] R. Bartoldus,[67] P. Bechtle,[67] J. F. Benitez,[67] R. Cenci,[67] J. P. Coleman,[67] M. R. Convery,[67] J. C. Dingfelder,[67] J. Dorfan,[67] G. P. Dubois-Felsmann,[67] W. Dunwoodie,[67] R. C. Field,[67] S. J. Gowdy,[67] M. T. Graham,[67] P. Grenier,[67] C. Hast,[67] W. R. Innes,[67] J. Kaminski,[67] M. H. Kelsey,[67] H. Kim,[67] P. Kim,[67] M. L. Kocian,[67] D. W. G. S. Leith,[67] S. Li,[67] B. Lindquist,[67] S. Luitz,[67] V. Luth,[67] H. L. Lynch,[67] D. B. MacFarlane,[67] H. Marsiske,[67] R. Messner,[67] D. R. Muller,[67] H. Neal,[67] S. Nelson,[67] C. P. O'Grady,[67] I. Ofte,[67] A. Perazzo,[67] M. Perl,[67] B. N. Ratcliff,[67] A. Roodman,[67] A. A. Salnikov,[67] R. H. Schindler,[67] J. Schwiening,[67] A. Snyder,[67] D. Su,[67] M. K. Sullivan,[67] K. Suzuki,[67] S. K. Swain,[67] J. M. Thompson,[67] J. Va'vra,[67] A. P. Wagner,[67] M. Weaver,[67] C. A. West,[67] W. J. Wisniewski,[67] M. Wittgen,[67] D. H. Wright,[67] H. W. Wulsin,[67] A. K. Yarritu,[67] K. Yi,[67] C. C. Young,[67] V. Ziegler,[67] P. R. Burchat,[68] A. J. Edwards,[68] S. A. Majewski,[68] T. S. Miyashita,[68] B. A. Petersen,[68] L. Wilden,[68] S. Ahmed,[69] M. S. Alam,[69] R. Bula,[69] J. A. Ernst,[69] B. Pan,[69] M. A. Saeed,[69] S. B. Zain,[69] S. M. Spanier,[70] B. J. Wogsland,[70] R. Eckmann,[71] J. L. Ritchie,[71] A. M. Ruland,[71] C. J. Schilling,[71] R. F. Schwitters,[71] B. W. Drummond,[72] J. M. Izen,[72] X. C. Lou,[72] S. Ye,[72] F. Bianchi,[73] D. Gamba,[73] M. Pelliccioni,[73] M. Bomben,[74] L. Bosisio,[74] C. Cartaro,[74] G. Della Ricca,[74] L. Lanceri,[74] L. Vitale,[74] V. Azzolini,[75] N. Lopez-March,[75] F. Martinez-Vidal,[75] D. A. Milanes,[75] A. Oyanguren,[75] J. Albert,[76] Sw. Banerjee,[76] B. Bhuyan,[76] H. H. F. Choi,[76] K. Hamano,[76] R. Kowalewski,[76] M. J. Lewczuk,[76] I. M. Nugent,[76] J. M. Roney,[76] R. J. Sobie,[76] T. J. Gershon,[77] P. F. Harrison,[77] J. Ilic,[77] T. E. Latham,[77] G. B. Mohanty,[77] H. R. Band,[78] X. Chen,[78] S. Dasu,[78] K. T. Flood,[78] Y. Pan,[78] M. Pierini,[78] R. Prepost,[78] C. O. Vuosalo,[78] and S. L. Wu[78]

(*BABAR* Collaboration)

[1]*Laboratoire de Physique des Particules, IN2P3/CNRS et Université de Savoie, F-74941 Annecy-Le-Vieux, France*
[2]*Universitat de Barcelona, Facultat de Fisica, Departament ECM, E-08028 Barcelona, Spain*
[3]*Università di Bari, Dipartimento di Fisica and INFN, I-70126 Bari, Italy*
[4]*University of Bergen, Institute of Physics, N-5007 Bergen, Norway*
[5]*Lawrence Berkeley National Laboratory and University of California, Berkeley, California 94720, USA*
[6]*University of Birmingham, Birmingham, B15 2TT, United Kingdom*
[7]*Ruhr Universität Bochum, Institut für Experimentalphysik 1, D-44780 Bochum, Germany*
[8]*University of Bristol, Bristol BS8 1TL, United Kingdom*
[9]*University of British Columbia, Vancouver, British Columbia, Canada V6T 1Z1*
[10]*Brunel University, Uxbridge, Middlesex UB8 3PH, United Kingdom*
[11]*Budker Institute of Nuclear Physics, Novosibirsk 630090, Russia*
[12]*University of California at Irvine, Irvine, California 92697, USA*
[13]*University of California at Los Angeles, Los Angeles, California 90024, USA*
[14]*University of California at Riverside, Riverside, California 92521, USA*
[15]*University of California at San Diego, La Jolla, California 92093, USA*
[16]*University of California at Santa Barbara, Santa Barbara, California 93106, USA*
[17]*University of California at Santa Cruz, Institute for Particle Physics, Santa Cruz, California 95064, USA*
[18]*California Institute of Technology, Pasadena, California 91125, USA*
[19]*University of Cincinnati, Cincinnati, Ohio 45221, USA*
[20]*University of Colorado, Boulder, Colorado 80309, USA*
[21]*Colorado State University, Fort Collins, Colorado 80523, USA*
[22]*Technische Universität Dortmund, Fakultät Physik, D-44221 Dortmund, Germany*
[23]*Technische Universität Dresden, Institut für Kern- und Teilchenphysik, D-01062 Dresden, Germany*
[24]*Laboratoire Leprince-Ringuet, CNRS/IN2P3, Ecole Polytechnique, F-91128 Palaiseau, France*
[25]*University of Edinburgh, Edinburgh EH9 3JZ, United Kingdom*
[26]*Università di Ferrara, Dipartimento di Fisica and INFN, I-44100 Ferrara, Italy*
[27]*Laboratori Nazionali di Frascati dell'INFN, I-00044 Frascati, Italy*
[28]*Università di Genova, Dipartimento di Fisica and INFN, I-16146 Genova, Italy*
[29]*Harvard University, Cambridge, Massachusetts 02138, USA*
[30]*Universität Heidelberg, Physikalisches Institut, Philosophenweg 12, D-69120 Heidelberg, Germany*
[31]*Imperial College London, London, SW7 2AZ, United Kingdom*

[32]University of Iowa, Iowa City, Iowa 52242, USA
[33]Iowa State University, Ames, Iowa 50011-3160, USA
[34]Johns Hopkins University, Baltimore, Maryland 21218, USA
[35]Universität Karlsruhe, Institut für Experimentelle Kernphysik, D-76021 Karlsruhe, Germany
[36]Laboratoire de l'Accélérateur Linéaire, IN2P3/CNRS et Université Paris-Sud 11, Centre Scientifique d'Orsay, B. P. 34, F-91898 Orsay Cedex, France
[37]Lawrence Livermore National Laboratory, Livermore, California 94550, USA
[38]University of Liverpool, Liverpool L69 7ZE, United Kingdom
[39]Queen Mary, University of London, E1 4NS, United Kingdom
[40]University of London, Royal Holloway and Bedford New College, Egham, Surrey TW20 0EX, United Kingdom
[41]University of Louisville, Louisville, Kentucky 40292, USA
[42]University of Manchester, Manchester M13 9PL, United Kingdom
[43]University of Maryland, College Park, Maryland 20742, USA
[44]University of Massachusetts, Amherst, Massachusetts 01003, USA
[45]Massachusetts Institute of Technology, Laboratory for Nuclear Science, Cambridge, Massachusetts 02139, USA
[46]McGill University, Montréal, Québec, Canada H3A 2T8
[47]Università di Milano, Dipartimento di Fisica and INFN, I-20133 Milano, Italy
[48]University of Mississippi, University, Mississippi 38677, USA
[49]Université de Montréal, Physique des Particules, Montréal, Québec, Canada H3C 3J7
[50]Mount Holyoke College, South Hadley, Massachusetts 01075, USA
[51]Università di Napoli Federico II, Dipartimento di Scienze Fisiche and INFN, I-80126, Napoli, Italy
[52]NIKHEF, National Institute for Nuclear Physics and High Energy Physics, NL-1009 DB Amsterdam, The Netherlands
[53]University of Notre Dame, Notre Dame, Indiana 46556, USA
[54]Ohio State University, Columbus, Ohio 43210, USA
[55]University of Oregon, Eugene, Oregon 97403, USA
[56]Università di Padova, Dipartimento di Fisica and INFN, I-35131 Padova, Italy
[57]Laboratoire de Physique Nucléaire et de Hautes Energies, IN2P3/CNRS, Université Pierre et Marie Curie-Paris6, Université Denis Diderot-Paris7, F-75252 Paris, France
[58]University of Pennsylvania, Philadelphia, Pennsylvania 19104, USA
[59]Università di Perugia, Dipartimento di Fisica and INFN, I-06100 Perugia, Italy
[60]Università di Pisa, Dipartimento di Fisica, Scuola Normale Superiore and INFN, I-56127 Pisa, Italy
[61]Princeton University, Princeton, New Jersey 08544, USA
[62]Università di Roma La Sapienza, Dipartimento di Fisica and INFN, I-00185 Roma, Italy
[63]Universität Rostock, D-18051 Rostock, Germany
[64]Rutherford Appleton Laboratory, Chilton, Didcot, Oxon, OX11 0QX, United Kingdom
[65]DSM/Dapnia, CEA/Saclay, F-91191 Gif-sur-Yvette, France
[66]University of South Carolina, Columbia, South Carolina 29208, USA
[67]Stanford Linear Accelerator Center, Stanford, California 94309, USA
[68]Stanford University, Stanford, California 94305-4060, USA
[69]State University of New York, Albany, New York 12222, USA
[70]University of Tennessee, Knoxville, Tennessee 37996, USA
[71]University of Texas at Austin, Austin, Texas 78712, USA
[72]University of Texas at Dallas, Richardson, Texas 75083, USA
[73]Università di Torino, Dipartimento di Fisica Sperimentale and INFN, I-10125 Torino, Italy
[74]Università di Trieste, Dipartimento di Fisica and INFN, I-34127 Trieste, Italy
[75]IFIC, Universitat de Valencia-CSIC, E-46071 Valencia, Spain
[76]University of Victoria, Victoria, British Columbia, Canada V8W 3P6
[77]Department of Physics, University of Warwick, Coventry CV4 7AL, United Kingdom
[78]University of Wisconsin, Madison, Wisconsin 53706, USA
(Received 29 March 2008; published 11 August 2008)

We report the measurement of the branching fractions of the rare decays $B^0 \to D_s^{(*)+}\pi^-$, $B^0 \to D_s^{(*)+}\rho^-$, and $B^0 \to D_s^{(*)-}K^{(*)+}$ in a sample of $381 \times 10^6 \Upsilon(4S)$ decays into $B\overline{B}$ pairs collected with the *BABAR* detector at the PEP-II asymmetric-energy e^+e^- storage ring. We present evidence for the

[*]Deceased.
[+]Now at Temple University, Philadelphia, Pennsylvania 19122, USA.
[‡]Now at Tel Aviv University, Tel Aviv, 69978, Israel.
[§]Also with Università di Perugia, Dipartimento di Fisica, Perugia, Italy.
[‖]Also with Università di Sassari, Sassari, Italy.

decay $B^0 \to D_s^- K^{*+}$ and the vector-vector decays $B^0 \to D_s^{*+}\rho^-$ and $B^0 \to D_s^{*-}K^{*+}$, as well as the first measurement of the vector meson polarization in these decays. We also determine the ratios of the CKM-suppressed to CKM-favored amplitudes $r(D^{(*)}\pi)$ and $r(D^{(*)}\rho)$ in decays $B^0 \to D^{(*)\pm}\pi^{\mp}$ and $B^0 \to D^{(*)\pm}\rho^{\mp}$, and comment on the prospects for measuring the *CP* observable $\sin(2\beta+\gamma)$.

DOI: 10.1103/PhysRevD.78.032005 PACS numbers: 12.15.Hh, 11.30.Er, 13.25.Hw

I. INTRODUCTION

The Cabibbo-Kobayashi-Maskawa (CKM) quark flavor-mixing matrix [1] provides an elegant explanation of the origin of *CP* violation within the standard model. *CP* violation manifests itself as a nonzero area of the unitarity triangle [2]. While it is sufficient to measure one of the angles to demonstrate the existence of *CP* violation, the unitarity triangle needs to be overconstrained by experimental measurements in order to demonstrate that the CKM mechanism is the correct explanation of this phenomenon. Precision measurements of the sides and angles of the unitarity triangle are the focus of the physics program at the *B* factories. While several theoretically clean measurements of the angle β exist [3], constraining the other two angles α and γ is significantly more challenging. A theoretically clean measurement of $\sin(2\beta+\gamma)$ can be obtained from the study of the time evolution for $B^0 \to D^{(*)-}\pi^+$ [4] and $B^0 \to D^{(*)-}\rho^+$ decays, which are available in large samples at the *B* factories, and for the corresponding CKM-suppressed modes $B^0 \to D^{(*)+}\pi^-$ and $B^0 \to D^{(*)+}\rho^-$ [5]. Measurements of *CP* asymmetries in $B^0 \to D^{(*)\mp}\pi^{\pm}$ and $B^0 \to D^{\mp}\rho^{\pm}$ decays have recently been published [6,7].

The interpretation of *CP* asymmetries in $B^0 \to D^{(*)\mp}\pi^{\pm}$ decays as a measurement of $\sin(2\beta+\gamma)$ requires knowledge of the ratios of the decay amplitudes,

$$r(D^{(*)}\pi) = \left|\frac{A(B^0 \to D^{(*)+}\pi^-)}{A(B^0 \to D^{(*)-}\pi^+)}\right|. \quad (1)$$

However, direct measurements of the doubly Cabibbo-suppressed branching fractions $\mathcal{B}(B^0 \to D^{(*)+}\pi^-)$ and $\mathcal{B}(B^0 \to D^{(*)+}\rho^-)$ are not possible with the currently available data samples due to the presence of the copious background from $\bar{B}^0 \to D^{(*)+}\pi^-$, $D^{(*)+}\rho^-$. On the other hand, assuming SU(3) flavor symmetry, $r(D^{(*)}\pi)$ can be related to the branching fraction of the decay $B^0 \to D_s^{(*)+}\pi^-$ [5]:

$$r(D^{(*)}\pi) = \tan\theta_c \frac{f_{D^{(*)}}}{f_{D_s^{(*)}}} \sqrt{\frac{\mathcal{B}(B^0 \to D_s^{(*)+}\pi^-)}{\mathcal{B}(B^0 \to D^{(*)-}\pi^+)}}, \quad (2)$$

where θ_c is the Cabibbo angle, and $f_{D^{(*)}}/f_{D_s^{(*)}}$ is the ratio of $D^{(*)}$ and $D_s^{(*)}$ meson decay constants [8–10]. Other SU(3)-breaking effects are believed to affect $r(D^{(*)}\pi)$ by (10–15)% [11].

The dominant Feynman diagrams for the decays $B^0 \to D^{(*)-}\pi^+(\rho^+)$, $B^0 \to D^{(*)+}\pi^-(\rho^-)$, $B^0 \to D_s^{(*)+}\pi^-(\rho^-)$, and $B^0 \to D_s^{(*)-}K^{(*)+}$ are shown in Fig. 1. Since $B^0 \to D_s^{(*)+}\pi^-$ has four different quark flavors in the final state, a single amplitude contributes to the decay [Fig. 1(c)]. On the other hand, two diagrams contribute to $B^0 \to D^{(*)-}\pi^+$ and $B^0 \to D^{(*)+}\pi^-$: tree amplitudes [Figs. 1(a) and 1(b)] and color-suppressed direct *W*-exchange amplitudes [Figs. 1(d) and 1(e)]. The latter are assumed to be negligibly small in Eq. (2). The decays $B^0 \to D_s^{(*)-}K^+$ [Fig. 1(f)] probe the size of the *W*-exchange amplitudes relative to the dominant processes $B^0 \to D^{(*)-}\pi^+$.

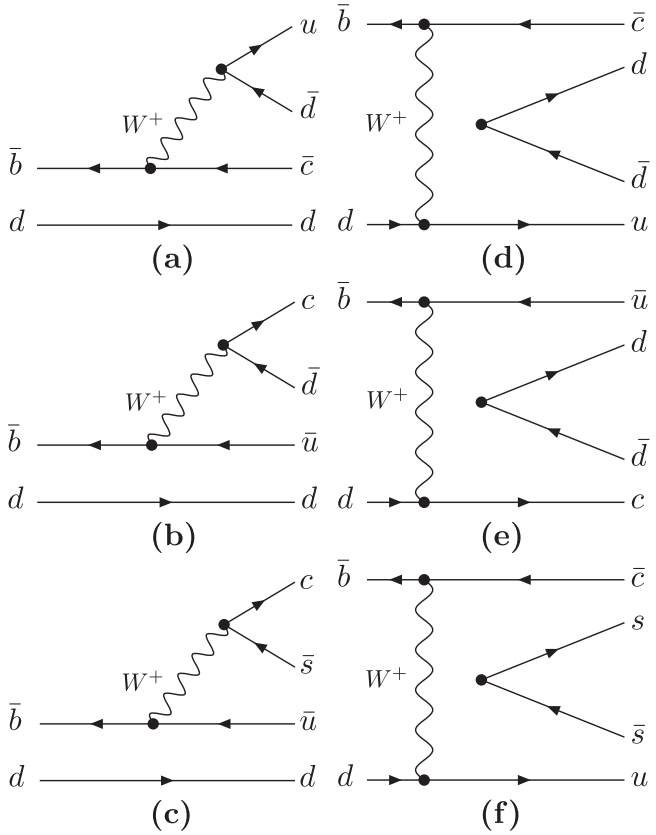

FIG. 1. Dominant Feynman diagrams for (a) CKM-favored decays $B^0 \to D^{(*)-}\pi^+(\rho^+)$, (b) doubly CKM-suppressed decays $B^0 \to D^{(*)+}\pi^-(\rho^-)$, and (c) the SU(3) flavor symmetry related decays $B^0 \to D_s^{(*)+}\pi^-(\rho^-)$; (d) the color-suppressed *W*-exchange contributions to $B^0 \to D^{(*)-}\pi^+(\rho^+)$, (e) $B^0 \to D^{(*)+}\pi^-(\rho^-)$, and (f) decay $B^0 \to D_s^{(*)-}K^{(*)+}$.

The rate of $B^0 \to D_s^{(*)-} K^{(*)+}$ decays could be enhanced by final state rescattering [12], in addition to the W-exchange amplitude. Such long-distance effects could also affect the vector meson polarization in $B^0 \to D_s^{*-} K^{*+}$ decays. The angular distribution in vector-vector decays $B^0 \to D_s^* V$ ($V = \rho$, K^*) is given by

$$\frac{d^2\Gamma}{d\cos\theta_{D_s^*} d\cos\theta_V} \propto [(1 - f_L)(1 + \cos^2\theta_{D_s^*})\sin^2\theta_V + 4 f_L \sin^2\theta_{D_s^*}\cos^2\theta_V], \quad (3)$$

where $\theta_{D_s^*}$ and θ_V are the helicity angles of D_s^{*+} and the vector meson V, respectively, $f_L = |A_0|^2/(\Sigma|A_\lambda|^2)$ is the longitudinal polarization fraction, and $A_{\lambda=-1,0,+1}$ are the helicity amplitudes. These distributions are integrated over the angle between the decay planes of D_s^{*+} and V.

For amplitudes dominated by the short-range (electroweak) currents, f_L is predicted to be near unity [13], with corrections of order $\mathcal{O}(m_V^2/m_B^2)$, where m_V is the mass of the vector meson produced by the weak current, and m_B is the mass of the B meson. Thus, the measurement of f_L can constrain the size of the long-distance contributions in $B^0 \to D_s^{*-} K^{*+}$ decays [12].

The branching fractions for the decays $B^0 \to D_s^{(*)+}\pi^-$, $B^0 \to D_s^{(*)+}\rho^-$, and $B^0 \to D_s^{(*)-} K^{(*)+}$ are estimated to be of order 10^{-5} [14]. The branching fractions $\mathcal{B}(B^0 \to D_s^{(*)+}\pi^-)$ and $\mathcal{B}(B^0 \to D_s^{(*)-} K^+)$ have been measured previously by the *BABAR* Collaboration [15]. In this paper we present the first evidence for the decays $B^0 \to D_s^{*+}\rho^-$ and $B^0 \to D_s^{(*)-} K^{*+}$, and a limit on the rate of $B^0 \to D_s^+\rho^-$. We also update the measurements of the branching fractions $\mathcal{B}(B^0 \to D_s^{(*)+}\pi^-)$ and $\mathcal{B}(B^0 \to D_s^{(*)-} K^+)$ with improved precision, using a 65% larger data set.

II. DATA SAMPLE AND THE DETECTOR

We use a sample of $381 \times 10^6 \Upsilon(4S)$ decays into $B\overline{B}$ pairs collected with the *BABAR* detector at the PEP-II asymmetric-energy e^+e^- collider [16]. A detailed description of the *BABAR* detector is available elsewhere [17]. The components of the detector crucial to this analysis are summarized below.

Charged-particle tracking is provided by a five-layer silicon vertex tracker (SVT) and a 40-layer drift chamber (DCH). For charged-particle identification, ionization energy loss (dE/dx) in the DCH and SVT, and Cherenkov radiation detected in a ring-imaging device (DIRC) are used. Photons and neutral pions are identified and measured using an electromagnetic calorimeter (EMC), which comprises 6580 thallium-doped CsI crystals. These systems are mounted inside a 1.5-Tesla solenoidal superconducting magnet. We use the GEANT4 [18] software to simulate interactions of particles traversing the *BABAR* detector, taking into account the varying detector conditions and beam backgrounds.

III. EVENT SELECTION AND ANALYSIS

The selection of events of interest proceeds in two steps. First, we preselect events with at least three reconstructed charged-particle tracks and a total measured energy greater than 4.5 GeV, as determined using all charged particles and neutral particles with energy above 30 MeV. In order to suppress $e^+e^- \to q\bar{q}$ ($q = u$, d, s, c) continuum background, the ratio of the second to zeroth order Fox-Wolfram moments [19] must be less than 0.5. In the second step of the selection process, we identify events of interest on the basis of the likelihood-based multivariate discriminant. Finally, we determine the yields of signal and background events in a maximum likelihood fit to the subset of the kinematic variables not used in the multivariate discriminant.

Candidates for D_s^+ mesons are reconstructed in the $D_s^+ \to \phi\pi^+$, $K_S^0 K^+$, and $\overline{K}^{*0}K^+$ final states, with $\phi \to K^+K^-$, $K_S^0 \to \pi^+\pi^-$, and $\overline{K}^{*0} \to K^-\pi^+$. The K_S^0 candidates are reconstructed from two oppositely charged tracks, and their momentum is required to make an angle $|\theta_{\rm flight}| < 11^\circ$ with the line connecting their vertex and the e^+e^- interaction point. All other tracks are required to originate from the e^+e^- interaction region, loosely defined by $|d_0| < 1.5$ cm and $|z_0| < 10$ cm, where d_0 and z_0 are the distances of closest approach to the primary e^+e^- vertex in the directions perpendicular and parallel to the beams, respectively. In order to reject background from $D^+ \to K_S^0\pi^+$ or $\overline{K}^{*0}\pi^+$, the K^+ candidate in the reconstruction of $D_s^+ \to K_S^0 K^+$ or $\overline{K}^{*0}K^+$ is required to satisfy positive kaon identification criteria, which have an efficiency of 85% and a 5% pion misidentification probability. The same selection is used to identify kaon daughters of the B^0 and K^{*+} mesons in decays $B^0 \to D_s^{(*)-} K^{(*)+}$. The selection is based on the ratios of likelihoods for kaon, pion, and proton identification in the SVT, DCH, and DIRC. The detector likelihoods are calibrated over a wide range of momenta using particles identified kinematically in clean decay chains, such as $D^{*+} \to D^0\pi^+$, $D^0 \to K^-\pi^+$, and $\Lambda \to p\pi^-$. In $\phi \to K^+K^-$ and $\overline{K}^{*0} \to K^-\pi^+$ decays, kaons are not positively identified, but instead candidates passing a likelihood-based pion selection are rejected. The selection efficiency of this "pion veto" is 95% for the kaons and 20% for the pions. Pion daughters of B^0 and ρ^- mesons in the $B^0 \to D_s^{(*)+}\pi^-$ and $B^0 \to D_s^{(*)+}\rho^-$ decays are required to be positively identified. Decay products of ϕ, $\overline{K}^{*0}$, D_s^+, and B^0 candidates are constrained to originate from a single vertex.

We reconstruct $\rho^+ \to \pi^+\pi^0$ candidates by combining a well-identified charged pion with a $\pi^0 \to \gamma\gamma$ candidate. The K^{*+} candidates are reconstructed through the decays $K^{*+} \to K^+\pi^0$ and $K^{*+} \to K_S^0\pi^+$. The neutral pion candidates are reconstructed from pairs of photons each with a minimum energy of 30 MeV. The invariant mass of the photon pair is required to be within ± 25 MeV/c^2 of the

nominal value [20]. The selected candidates are constrained to the nominal π^0 mass before forming the ρ^+ or K^{*+} candidates. We require that the invariant mass of the two pions forming the ρ^- candidate be within ± 320 MeV$/c^2$ of the nominal value [20], and that the invariant mass of the $K^+\pi^0$ and $K^0_S\pi^+$ pairs be within ± 75 MeV$/c^2$ of the nominal K^{*+} mass [20]. $K^0_S\pi^+$ pairs are constrained to a common geometric vertex.

We reconstruct D_s^{*+} candidates in the mode $D_s^{*+} \to D_s^+\gamma$ by combining D_s^+ and photon candidates. Photon candidates are required to have a lateral energy profile in the EMC consistent with a photon shower, and to have an energy greater than 100 MeV in the laboratory frame. When forming a D_s^{*+}, the D_s^+ candidate is required to have an invariant mass within 10 MeV$/c^2$ of the nominal value [20]. For $B^0 \to D_s^{*+}\rho^-$ and $B^0 \to D_s^{*-}K^{*+}$ modes, we apply a "π^0 veto" by rejecting photons that, in combination with any other photon in the event, form an invariant mass that falls within $125 < m_{\gamma\gamma} < 145$ MeV$/c^2$.

The efficiency of the initial preselection discussed above varies between 14% ($B^0 \to D_s^{*+}\rho^-$, $D_s^+ \to \overline{K}^{*0}K^+$) and 48% ($B^0 \to D_s^+\pi^-$, $D_s^+ \to \phi\pi^+$). After the preselection, we identify signal B decay candidates using a likelihood ratio $R_L = \mathcal{L}_{\rm sig}/(\mathcal{L}_{\rm sig} + \mathcal{L}_{\rm bkg})$, where $\mathcal{L}_{\rm sig} = \prod_j \mathcal{P}_{\rm sig}(x_k)$ is the multivariate likelihood for the signal hypothesis and $\mathcal{L}_{\rm bkg} = \prod_i \mathcal{P}_{\rm bkg}(x_k)$ is the likelihood for the background hypothesis. Here x_k represents one of the discriminating variables described below, which are computed for each event. The likelihoods for the signal and background hypotheses are computed as a product of the probability density functions (PDFs) $\mathcal{P}_{\rm sig}(x_k)$ and $\mathcal{P}_{\rm bkg}(x_k)$, respectively, for the following selection variables: invariant masses of the ϕ, $\overline{K}^{*0}$, ρ^+, K^{*+}, and K^0_S candidates; χ^2 confidence level of the vertex fit for the B^0 and D_s^+ mesons; the helicity angles of the ϕ, $\overline{K}^{*0}$, ρ^+, K^{*+}, and D_s^{*+} meson decays; the mass difference $\Delta m(D_s^{*+}) = m(D_s^{*+}) - m(D_s^+)$; the polar angle θ_B of the B candidate momentum vector with respect to the beam axis in the e^+e^- center-of-mass (c.m.) frame; the angle θ_T between the thrust axis of the B candidate and the thrust axis of all other particles in the event in the c.m. frame; the event topology variable $\mathcal{F}$; and the kinematic variable ΔE described below. Correlations among these variables are small.

The helicity angle θ_H is defined as the angle between one of the decay products of a meson and the flight direction of its parent particle in the meson's rest frame. Polarization of the vector mesons in the signal decays causes the cosines of their helicity angles to be distributed as $\cos^2\theta_H$ (ϕ, $\overline{K}^{*0}$, ρ^+, and K^{*+}) or $1 - \cos^2\theta_H$ (D_s^{*+}), while the random background combinations tend to produce a more uniform distribution in $\cos\theta_H$, with a peak in the forward direction (which corresponds to a low-energy π^0) for ρ^+ and K^{*+} candidates. We do not include the helicity angles for D_s^{*+}, ρ^+, and K^{*+} mesons in the likelihood ratio R_L for the vector-vector $B^0 \to D_s^{*+}\rho^-$ and $B^0 \to D_s^{*-}K^{*+}$ modes, since the polarizations of the vector mesons in these decays are not known *a priori*. Instead, the helicity angles are used in the multidimensional likelihood fit to determine the polarizations, as discussed below.

The variables $\cos\theta_B$, $\cos\theta_T$, and $\mathcal{F}$ discriminate between spherically symmetric $B\overline{B}$ events and jetlike continuum background using event topology. The polar angle θ_B is distributed as $\sin^2\theta_B$ for real B decays, while being nearly flat in $\cos\theta_B$ for the continuum. $B\overline{B}$ pairs form a nearly uniform $|\cos\theta_T|$ distribution, while the $|\cos\theta_T|$ distribution for continuum events peaks at 1. A linear (Fisher) discriminant $\mathcal{F}$ is derived from the values of sphericity and thrust for the event, and the two Legendre moments L_0 and L_2 of the energy flow around the B-candidate thrust axis [21].

The ratio R_L has a maximum at $R_L = 1$ for signal events, and at $R_L = 0$ for background originating from continuum events. It also discriminates well against B decays without a real D_s^+ meson in the final state. The Monte Carlo (MC) simulated distributions of the R_L variable for signal and background events, in $B^0 \to D_s^+\pi^-$ decays, are shown in Fig. 2.

Finally, two other variables $m_{\rm ES}$ and ΔE take advantage of the unique kinematic properties of the $e^+e^- \to \Upsilon(4S) \to B\overline{B}$ decays. The beam energy spread is significantly smaller than the energy resolution of the reconstructed B mesons and, at the same time, larger than the momentum resolution. The momentum of the signal candidates is included in the beam-energy-substituted mass $m_{\rm ES} = \sqrt{(s/2 + \mathbf{p}_i \cdot \mathbf{p}_B)^2/E_i^2 - \mathbf{p}_B^2}$, where $\sqrt{s}$ is the total c.m. energy, $(E_i, \mathbf{p}_i)$ is the four-momentum of the initial e^+e^- system, and $\mathbf{p}_B$ is the B^0 candidate momentum, both measured in the laboratory frame. The second variable is $\Delta E = E_B^* - \sqrt{s}/2$, where E_B^* is the B^0 candidate energy in the c.m. frame. For signal events, the $m_{\rm ES}$ distribution is nearly Gaussian and centered at the B meson mass with a resolution of about (2.5–2.8) MeV$/c^2$, and the ΔE distribution has a maximum near zero with a resolution of (17–25) MeV. We include ΔE in the definition of the likelihood

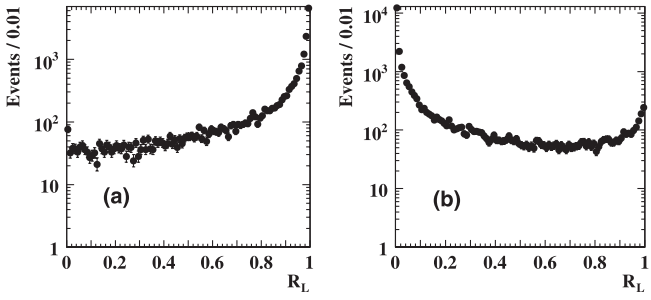

FIG. 2. Distribution of the likelihood ratio R_L for the mode $B^0 \to D_s^+\pi^-$, $D_s^+ \to \phi\pi^+$. Shown are (a) the simulated signal events, and (b) the sum of the simulated background samples from the B^0 and B^+ decays, and $e^+e^- \to q\bar{q}$ events.

ratio R_L; $m_{\rm ES}$ is used as a discriminating variable in the maximum likelihood fit described below.

We parametrize the signal and background PDFs using large samples of simulated events. We select $B^0 \to D_s^{(*)+}\pi^-$ and $B^0 \to D_s^{(*)-}K^+$ candidates that satisfy $R_L > 0.85$, and accept $B^0 \to D_s^{(*)+}\rho^-$ and $B^0 \to D_s^{(*)-}K^{*+}$ candidates with $R_L > 0.96$. We measure the relative efficiencies ε_{R_L} of the R_L selections in copious data samples of decays $B^0 \to D^-\pi^+$, $D^-\rho^+$ ($D^- \to K^+\pi^-\pi^-$, $K^0_S\pi^-$) and $B^+ \to \overline{D}^{*0}\pi^+$, $\overline{D}^{*0}\rho^+$ ($\overline{D}^{*0} \to \overline{D}^0\gamma$, $D^0 \to K^-\pi^+$) in which the kinematics is similar to those of our signal events, and find that they are consistent with Monte Carlo estimates of $\varepsilon_{R_L} \approx 70\%(40\%)$ for $B^0 \to D_s^{(*)+}\pi^-$ and $B^0 \to D_s^{(*)-}K^+$ ($B^0 \to D_s^{(*)+}\rho^-$ and $B^0 \to D_s^{(*)-}K^{*+}$) modes. The fraction of continuum background events passing the selection varies between 2% and 15%, depending on the mode.

Less than 30% of the selected events in the $B^0 \to D_s^{*+}\pi^-$, $B^0 \to D_s^{*-}K^+$, $B^0 \to D_s^{(*)+}\rho^-$, and $B^0 \to D_s^{(*)-}K^{*+}$ channels ($< 2\%$ in $B^0 \to D_s^+\pi^-$ and $B^0 \to D_s^-K^+$) contain two or more candidates that satisfy the criteria listed above. In such events we select a single B^0 candidate based on an event χ^2 formed from ΔE, $m(D_s)$ and (where appropriate) $\Delta m(D_s^{*+})$, $m(\rho)$, $m(K^*)$, $m(\pi^0)$, and $m(K^0_S)$, and their uncertainties.

IV. EXTRACTION OF SIGNAL YIELDS

After the R_L requirement is applied, we define the region of interest using the beam-energy-substituted mass $m_{\rm ES}$ and the mass of the D_s^+ candidate $m(D_s)$. We require $5.2 < m_{\rm ES} < 5.3$ GeV/c^2 and $|m(D_s) - m(D_s)_{\rm PDG}| < 50$ MeV/c^2 for $B^0 \to D_s^+\pi^-$, $B^0 \to D_s^+\rho^-$, and $B^0 \to D_s^-K^{(*)+}$ modes, where $m(D_s)_{\rm PDG}$ is the world average D_s mass [20]. The invariant mass $m(D_s)$ has a resolution of (5–6) MeV/c^2, depending on the D_s^+ decay mode. The selection is significantly broader than the region populated by the signal events, and allows us to constrain backgrounds in the signal region. For $B^0 \to D_s^{*+}\pi^-$, $B^0 \to D_s^{*+}\rho^-$, and $B^0 \to D_s^{*-}K^{(*)+}$, we require $|m(D_s) - m(D_s)_{\rm PDG}| < 10$ MeV/c^2.

Five classes of background events contribute to the fit region. First is the *combinatorial background*, in which a true or fake $D_s^{(*)}$ candidate is combined with a randomly selected light meson. Second, B meson decays such as $\bar{B}^0 \to D^{(*)+}\pi^-$ or $\bar{B}^0 \to D^{(*)+}\rho^-$ with $D^+ \to K^0_S\pi^+$ or $\bar{K}^{*0}\pi^+$ can constitute a background for the $B^0 \to D_s^{(*)+}\pi^-$ and $B^0 \to D_s^{(*)+}\rho^-$ modes if the pion in the D decay is misidentified as a kaon (*reflection background*). The reflection background has nearly the same $m_{\rm ES}$ distribution as the signal but different distributions in ΔE and $m(D_s)$. The corresponding backgrounds for the $B^0 \to D_s^-K^{(*)+}$ mode ($B^0 \to D^-K^{(*)+}$) are negligible. Third, rare *charmless B* decays into the same final state, such as $B^0 \to \overline{K}^{(*)0}K^+h$ (where $h = \pi$, ρ, K, or K^*), have the same $m_{\rm ES}$ and ΔE distributions as the $B^0 \to D_sh$ signal, but are nearly flat in $m(D_s)$. The charmless background is significant in $B^0 \to D_s^+\pi^-$, $B^0 \to D_s^+\rho^-$, and $B^0 \to D_s^-K^{(*)+}$ decays, but is effectively rejected by the $\Delta m(D_s^{*+})$ variable for the modes with D_s^{*+}.

Finally, two classes of background events have nearly the same distribution as the signal events in both $m(D_s)$ and $m_{\rm ES}$. For $B^0 \to D_s^{(*)-}K^{*+}$ modes we take into account the potential contributions from the *nonresonant* decays $B^0 \to D_s^{(*)-}K^0\pi^+$ (which have recently been observed [22]) and color-suppressed $B^0 \to D_s^{(*)-}K^+\pi^0$ (unobserved so far). Analogous nonresonant modes $B^0 \to D_s^{(*)+}\pi^-\pi^0$ require the additional popping of a color-matched $q\bar{q}$ pair. They are expected to be small compared to $B^0 \to D_s^{(*)+}\rho^-$ [22] and are ignored. Finally, *crossfeed background* from misidentification of $\overline{B}^0 \to D_s^{(*)-}\pi^+$ events as $B^0 \to D_s^{(*)-}K^+$ signal, and vice versa, needs to be taken into account.

For each mode of interest, we perform an unbinned extended maximum likelihood (ML) fit to separate the signal events from the backgrounds and extract the signal branching fractions. For $B^0 \to D_s^+\pi^-$, $B^0 \to D_s^+\rho^-$, $B^0 \to D_s^-K^+$, and $B^0 \to D_s^-K^{*+}$, we perform a two-dimensional fit to the $m_{\rm ES}$ and $m(D_s)$ distributions. For $B^0 \to D_s^{*+}\pi^-$ and $B^0 \to D_s^{*-}K^+$ decays, we fit the one-dimensional $m_{\rm ES}$ distribution. In vector-vector modes $B^0 \to D_s^{*+}\rho^-$ and $B^0 \to D_s^{*-}K^{*+}$, we determine both the branching fractions of the signal modes and the polarization of the vector mesons by performing a three-dimensional fit to the distribution of $m_{\rm ES}$, and the two helicity angles of the D_s^{*+} and ρ^- (K^{*+}) mesons.

For each B decay, we simultaneously fit distributions in the three D_s^+ decay modes, constraining the signal branching fractions to a common value. The likelihood function contains the contributions of the signal and the five background components discussed above. The function to be maximized is

$$\mathcal{L} = \exp\left(-\sum_{k,m} n_{km}\right)\prod_{i=1}^{N_{\rm cand}}\left(\sum_j n_{jm}\mathcal{P}_{jm}(\vec{\zeta}_i)\right) \qquad (4)$$

where n_{jm} is the number of events for each event type j (signal and all background modes) in each D_s decay mode m, and $\mathcal{P}_{jm}(\vec{\zeta}_i)$ is the probability density function of the variables $\vec{\zeta}_i = (m_{\rm ES}, m(D_s), \cos\theta_{D_s^*}, \cos\theta_V)$ for the ith event. The likelihood product is computed over all candidates $N_{\rm cand}$ in the region of interest. We parametrize the event yields as

$$n_{jm} = N_{B\overline{B}}\mathcal{B}_j\mathcal{B}_m^{Ds}\varepsilon_{jm}, \qquad (5)$$

where m stands for $D_s^+ \to \phi\pi^+$, $D_s^+ \to \overline{K}^{*0}K^+$, or $D_s^+ \to K^0_SK^+$, $N_{B\overline{B}} = 381 \times 10^6$, $\mathcal{B}_j$ is the B decay branching fraction, $\mathcal{B}_m^{Ds}$ is the branching fraction of the mth D_s^+

mode, and ε_{jm} is the reconstruction efficiency. For $D_s^+ \to \phi\pi^+$ and $D_s^+ \to \bar{K}^{*0}K^+$ branching fractions, we use the current world average values [20], while for $\mathcal{B}(D_s^+ \to K_S^0 K^+)$ we take advantage of the most recent measurement from the CLEO Collaboration [23], which differs from the previously reported central value [20] by about 50%:

$$\mathcal{B}(D_s^+ \to \phi\pi^+, \phi \to K^+K^-) = (2.20 \pm 0.20)\%,$$
$$\mathcal{B}(D_s^+ \to \overline{K}^{*0}K^+, \overline{K}^{*0} \to K^-\pi^+) = (2.5 \pm 0.5)\%,$$
$$\mathcal{B}(D_s^+ \to K_S^0 K^+, K_S^0 \to \pi^+\pi^-) = (1.04 \pm 0.07)\%.$$

The branching fractions of the channels contributing to the reflection background are fixed in the fit to the current world average values [20], and the branching fractions of the crossfeed backgrounds are determined by iterating the fits over each B decay mode. The branching fractions of the nonresonant backgrounds are fixed to the values recently measured by *BABAR* [22]. In the case of $B^0 \to D_s^{(*)-}K^+\pi^0$, which can contribute to $B^0 \to D_s^{(*)-}K^{*+}$ ($K^{*+} \to K^+\pi^0$), we estimate the branching fraction by

$$\mathcal{B}(B^0 \to D_s^{(*)-}K^+\pi^0) \approx \mathcal{B}(B^+ \to D_s^{(*)-}K^+\pi^+)\frac{\mathcal{B}(B^0 \to \bar{D}^0\pi^0)}{\mathcal{B}(B^+ \to \bar{D}^0\pi^+)}. \quad (6)$$

This scaling assumes that the dominant mechanism for producing both $D_s^{(*)-}K^+\pi^0$ and $D_s^{(*)-}K^+\pi^+$ final states is a subthreshold production of a charmed D^{**0} meson, which subsequently decays into $D_s^{(*)-}K^+$, as indicated by the invariant mass spectrum of $D_s^{(*)-}K^+$ [22]. Since the decay $B^0 \to D^{**0}\pi^0$ is color suppressed compared to $B^+ \to D^{**0}\pi^+$, we estimate the color-suppression factor from the $B^0 \to \bar{D}^0\pi^0$ decays. Direct production of the color-suppressed $D_s^{(*)-}K^+\pi^0$ final state (without the intermediate D^{**0}) results in a smaller branching fraction estimate. We assign a 100% systematic uncertainty to $\mathcal{B}(B^0 \to D_s^{(*)-}K^+\pi^0)$.

The expected yields of the dominant B-decay backgrounds are listed in Table I.

The PDFs and efficiencies for the signal, reflection, and crossfeed backgrounds are determined independently for

TABLE I. Expected background yields from the dominant B decay modes, fixed in the likelihood fit.

Signal mode	Background mode	$N(D_s^+ \to \phi\pi^+)$	$N(D_s^+ \to \overline{K}^{*0}K^+)$	$N(D_s^+ \to K_S^0K^+)$
$B^0 \to D_s^+\pi^-$	$B^0 \to D_s^-K^+$	1.4 ± 0.2	0.4 ± 0.1	0.3 ± 0.1
	$B^0 \to D^-\pi^+$	15.4 ± 1.2	19.5 ± 1.5	13.0 ± 1.0
$B^0 \to D_s^{*+}\pi^-$	$B^0 \to D_s^{*-}K^+$	0.9 ± 0.2	0.3 ± 0.1	0.3 ± 0.1
	$B^0 \to D^-\rho^+$	0.5 ± 0.2	3.4 ± 0.6	1.7 ± 0.4
	$B^0 \to D^{*-}\pi^+$, $D^{*-} \to D^-\pi^0$	0.3 ± 0.1	1.1 ± 0.2	0.7 ± 0.1
$B^0 \to D_s^+\rho^-$	$B^0 \to D_s^{*+}\rho^-$	6.6 ± 2.0	1.3 ± 0.5	1.5 ± 0.5
	$B^0 \to D_s^{*+}\pi^-$	6.0 ± 1.3	1.2 ± 0.4	1.5 ± 0.3
	$B^+ \to D_s^{*+}\pi^0$	3.7 ± 0.8	1.0 ± 0.3	1.0 ± 0.2
	$B^0 \to D^-\rho^+$	24.4 ± 4.2	33.1 ± 5.7	28.8 ± 4.9
	$B^0 \to D^{*-}\rho^+$, $D^{*-} \to D^0\pi$	0.3 ± 0.2	5.4 ± 3.3	8.2 ± 1.4
	$B^0 \to D^{*-}\rho^+$, $D^{*-} \to D^-\pi^0$	0.8 ± 0.4	1.4 ± 0.6	2.1 ± 0.5
$B^0 \to D_s^{*+}\rho^-$	$B^0 \to D^-\rho^+$	0.7 ± 0.2	1.6 ± 0.4	2.5 ± 0.8
	$B^0 \to D^{*-}\rho^{*+}$, $D^{*-} \to D^-\pi^0$	0.1 ± 0.0	0.7 ± 0.2	0.8 ± 0.1
$B^0 \to D_s^-K^+$	$B^0 \to D_s^+\pi^-$	0.6 ± 0.1	0.3 ± 0.1	0.2 ± 0.0
	$B^0 \to D_s^{*-}K^+$	1.3 ± 0.3	0.3 ± 0.1	0.2 ± 0.0
	$B^0 \to D^-K^+$	0.9 ± 0.3	2.1 ± 0.7	1.3 ± 0.4
$B^0 \to D_s^{*-}K^+$	$B^0 \to D_s^-K^+$	0.9 ± 0.2	0.2 ± 0.0	0.1 ± 0.0
	$B^0 \to D_s^-K^{*+}$	0.8 ± 0.3	0.3 ± 0.1	0.2 ± 0.1
	$B^0 \to D_s^{*+}\pi^-$	0.4 ± 0.1	0.2 ± 0.0	0.2 ± 0.0
$B^0 \to D_s^-K^{*+}$, $K^{*+} \to K_S^0\pi^+$	$B^0 \to D_s^{*-}K^{*+}$	0.3 ± 0.1	0.1 ± 0.0	0.0 ± 0.0
	$B^0 \to D_s^-\pi^+K^0$	1.8 ± 0.7	0.7 ± 0.3	0.6 ± 0.2
$B^0 \to D_s^-K^{*+}$, $K^{*+} \to K^+\pi^0$	$B^0 \to D_s^{*-}K^+$	2.5 ± 0.5	0.9 ± 0.2	0.9 ± 0.2
	$B^0 \to D_s^{*-}K^{*+}$	1.0 ± 0.5	0.3 ± 0.2	0.4 ± 0.2
	$B^0 \to D_s^-K^+\pi^0$	0.4 ± 0.4	0.1 ± 0.1	0.1 ± 0.1
$B^0 \to D_s^{*-}K^{*+}$, $K^{*+} \to K_S^0\pi^+$	$B^0 \to D_s^-K^{*+}$	0.1 ± 0.0	0.0 ± 0.0	0.0 ± 0.0
	$B^0 \to D_s^{*-}\pi^+K^0$	0.6 ± 0.4	0.2 ± 0.2	0.2 ± 0.1
$B^0 \to D_s^{*-}K^{*+}$, $K^{*+} \to K^+\pi^0$	$B^0 \to D_s^-K^{*+}$	0.4 ± 0.1	0.1 ± 0.0	0.2 ± 0.1
	$B^0 \to D_s^{*-}K^+\pi^0$	0.1 ± 0.1	0.0 ± 0.0	0.0 ± 0.0

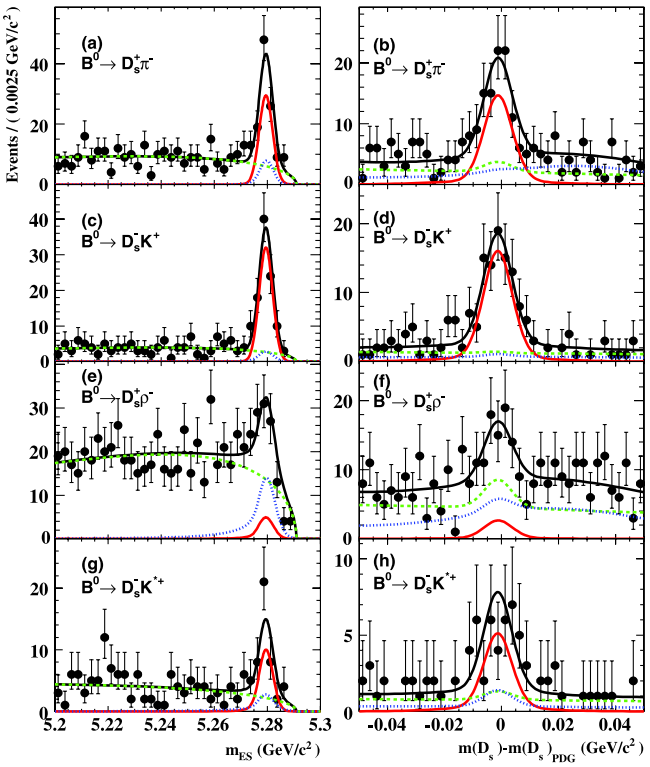

FIG. 3 (color online). (a,c,e,g) $m_{\rm ES}$ projection of the fit with $|m(D_s^+) - m(D_s^+)_{\rm PDG}| < 10$ MeV/c^2; and (b,d,f,h) $m(D_s)$ projection with $5.275 < m_{\rm ES} < 5.285$ GeV/c^2 for (a, b) $B^0 \to D_s^+\pi^-$, (c,d) $B^0 \to D_s^- K^+$, (e,f) $B^0 \to D_s^+\rho^-$, and (g,h) $B^0 \to D_s^- K^{*+}$. The black solid curves correspond to the full PDF from the combined fit to all D_s^+ decay modes. Individual contributions are shown as solid red (signal), green dashed (combinatorial background), and blue dotted (sum of reflection, charmless, crossfeed, and nonresonant backgrounds) curves.

each D_s^+ decay mode using Monte Carlo samples. The signal contribution is modeled as a Gaussian ($B^0 \to D_s^+\pi^-$ and $B^0 \to D_s^- K^+$) or a "Crystal Ball" function [24] in $m_{\rm ES}$ and a double Gaussian in $m(D_s)$. The combinatorial background is described in $m_{\rm ES}$ by a threshold function [25], $dN/dx \propto x\sqrt{1-2x^2/s}\exp[-\xi(1-2x^2/s)]$, characterized by the shape parameter ξ. This shape parameter, common to all D_s^+ modes, is allowed to vary in the fit. In $m(D_s)$, the combinatorial background is well described by a combination of a first-order polynomial (fake D_s^+ candidates) and a Gaussian with (5–6) MeV/c^2 resolution (true D_s^+ candidates). The charmless background is parametrized by the signal Gaussian shape in $m_{\rm ES}$ and a first-order polynomial in $m(D_s)$.

Ideally, the distribution of the helicity angles in the vector-vector decays is given by Eq. (3). The helicity angle $\theta_{D_s^*}$ is defined as the angle between the direction of the photon in $D_s^* \to D_s\gamma$ and the direction of the B in the rest frame of the D_s^* candidate. The helicity angle θ_V is similarly defined by the direction of the charged daughter particle in the decays $\rho^+ \to \pi^+\pi^0$, $K^{*+} \to K^+\pi^0$, and $K^{*+} \to K_S^0\pi^+$. Since the momenta of the decay products in the laboratory frame depend on the helicity angles, acceptance and efficiency effects modify the ideal angular distribution. We determine the PDFs of the signal events using the Monte Carlo simulation, and measure the angular distribution of the combinatorial background in the data region $m_{\rm ES} < 5.27$ GeV/c^2.

For $B^0 \to D_s^+\pi^-$, $B^0 \to D_s^+\rho^-$, and $B^0 \to D_s^- K^+$, the fit constrains 14 free parameters: the shape parameter of the combinatorial background ξ (1 parameter for all D_s^+ modes), the slopes of the combinatorial and charmless backgrounds in $m(D_s)$ (3 parameters), the fractions of true D_s^+ candidates in combinatorial background (3), the yields of combinatorial background events (3), the yields of charmless events (3), and the branching fraction of the signal mode (1). In the $B^0 \to D_s^- K^{*+}$ mode (6 individual submodes, spanning 3 D_s^+ channels and 2 K^{*+} channels), 26 free parameters are constrained. For the $B^0 \to D_s^{*+}\pi^-$ and $B^0 \to D_s^{*-} K^+$ decays, 5 free parameters are determined by the fit: ξ (1 parameter for all D_s^+ modes), the number of combinatorial background events (3), and the branching fraction of the signal mode (1). For $B^0 \to D_s^{*+}\rho^-$ and $B^0 \to D_s^{*-} K^{*+}$ fits, we add one more free parameter to the fit: the longitudinal polarization fraction

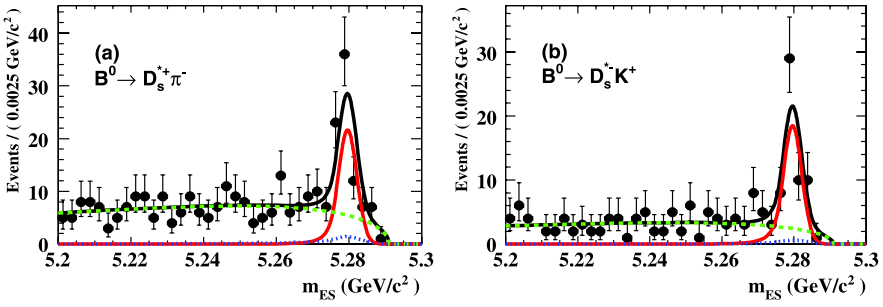

FIG. 4 (color online). $m_{\rm ES}$ projection of the fit for (a) $B^0 \to D_s^{*+}\pi^-$ and (b) $B^0 \to D_s^{*-} K^+$. The black solid curves correspond to the full PDF from the combined fit to all D_s^+ decay modes. Individual contributions are shown as solid red (signal), green dashed (combinatorial background), and blue dotted (sum of reflection, charmless, and crossfeed backgrounds) curves.

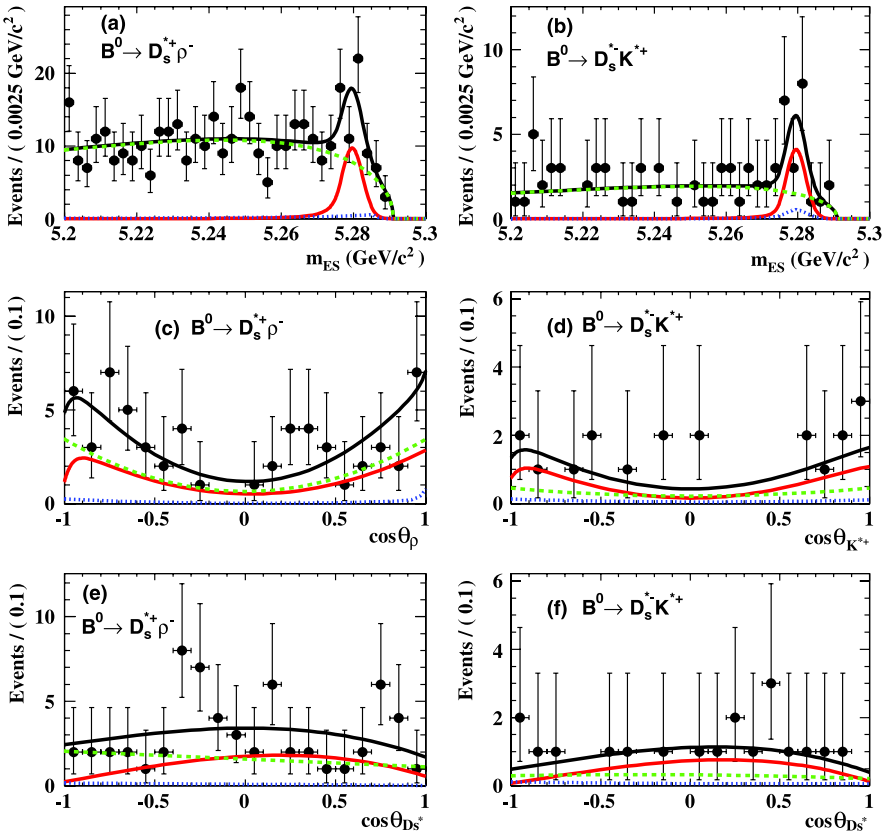

FIG. 5 (color online). Projections of the fit on to (a,b) $m_{\rm ES}$, (c) $\cos\theta_\rho$, (d) $\cos\theta_{K^*}$, and (e,f) $\cos\theta_{D_s^*}$ for (a,c,e) $B^0 \to D_s^{*+}\rho^-$ and (b,d, f) $B^0 \to D_s^{*-}K^{*+}$. For helicity projections, a selection $5.275 < m_{\rm ES} < 5.285$ GeV$/c^2$ is applied. The black solid curves correspond to the full PDF from the combined fit to all D_s^+ decay modes. Individual contributions are shown as solid red (signal), green dashed (combinatorial background), and blue dotted (sum of reflection, charmless, crossfeed, and nonresonant backgrounds) curves.

f_L [see Eq. (3)]. The total number of free parameters is 6 in $B^0 \to D_s^{*+}\rho^-$ and 9 in $B^0 \to D_s^{*-}K^{*+}$.

The results of the fits are shown in Figs. 3–5 and summarized in Table II.

V. SYSTEMATIC UNCERTAINTIES

For the branching fractions, the systematic errors are dominated by the 9% relative uncertainty for $\mathcal{B}(D_s^+ \to \phi\pi^+)$ [20]. The uncertainty in the branching fraction ratio $\mathcal{B}(D_s^+ \to \overline{K}^{*0}K^+)/\mathcal{B}(D_s^+ \to \phi\pi^+)$ contributes (2–4)%, depending on the decay channel, and the uncertainty in $\mathcal{B}(D_s^+ \to K_S^0 K^+)$ contributes (1–4)%. We estimate uncertainties due to modeling of the resonance (K^{*0}, ϕ, ρ, and K^{*+}) line shapes by measuring the effect of the line-shape variation on signal selection efficiency.

The uncertainties in the signal selection efficiency are determined by the accuracy with which the detector effects are modeled in the Monte Carlo simulations. Tracking, particle identification (PID), photon, π^0, and K_S^0 reconstruction efficiencies are measured across the wide range of particle momenta in the dedicated data control samples. The tracking efficiency and resolution are adequately reproduced by the simulations. The simulated distributions are corrected for the efficiency and resolution of the π^0 reconstruction. The efficiency of the R_L cut is also measured in the data control samples, as discussed in Section III.

The uncertainties due to the knowledge of the signal and background PDFs in the ML fit are estimated by measuring the variation of the fitted values of the branching fractions when PDF parameters are varied within their uncertainties. The correlations between parameters are taken into account. The uncertainties in the signal PDF parameters for the key discriminants ΔE, $m_{\rm ES}$, $\Delta m(D_s)$, $\Delta m(D_s^{*+})$, and $\cos\theta_{D_s^{*+}}$ are determined by comparing data and Monte Carlo simulations for the samples of decays $B^0 \to D^-\pi^+$, $D^-\rho^+$ ($D^- \to K^+\pi^-\pi^-$, $K_S^0\pi^-$) and $B^+ \to \overline{D}^{*0}\pi^+$, $\overline{D}^{*0}\rho^+$ ($\overline{D}^{*0} \to \overline{D}^0\gamma$, $D^0 \to K^-\pi^+$). The uncertainties in the signal PDFs for $\cos\theta_{\rho,K*}$ and the PDFs for the peaking backgrounds are determined by Monte Carlo simulations. These distributions depend on the modeling of the charged track and π^0 reconstruction, discussed above. The helicity angle PDFs for the continuum background are determined in the data sideband $m_{\rm ES} < 5.27$ GeV$/c^2$, and their uncertainties are statistical in nature.

TABLE II. The number of reconstructed candidates ($N_{\rm raw}$), the signal yield ($N_{\rm sig}$, computed from the fitted branching fractions), the combinatorial background ($N_{\rm comb}$), and the sum of charmless, reflection, nonresonant, and crossfeed contributions ($N_{\rm peak}$), extracted from the likelihood fit. Also given are the reconstruction efficiency (ε), the signal significance $\mathcal{S}$, the measured branching fraction $\mathcal{B}$, and the fraction of longitudinal polarization f_L (where appropriate). The first uncertainty is statistical, and the second is systematic.

B mode	D_s mode	$N_{\rm raw}$	$N_{\rm sig}$	$N_{\rm comb}$	$N_{\rm peak}$	$\varepsilon(\%)$	$\mathcal{S}$	$\mathcal{B}(10^{-5})$	f_L
$B^0 \to D_s^+ \pi^-$	$D_s^+ \to \phi\pi^+$	582	50 ± 9	500 ± 24	31 ± 10	25.2			
	$D_s^+ \to \overline{K}^{*0}K^+$	402	18 ± 5	352 ± 20	35 ± 8	8.0	8.2σ	$2.5 \pm 0.4 \pm 0.2$	
	$D_s^+ \to K_S^0K^+$	282	19 ± 3	246 ± 17	25 ± 7	19.4			
$B^0 \to D_s^{*+} \pi^-$	$D_s^+ \to \phi\pi^+$	150	33 ± 7	113 ± 12	1.6 ± 0.2	16.7			
	$D_s^+ \to \overline{K}^{*0}K^+$	96	12 ± 3	77 ± 10	4.8 ± 0.6	5.5	6.7σ	$2.6^{+0.5}_{-0.4} \pm 0.2$	
	$D_s^+ \to K_S^0K^+$	52	13 ± 3	41 ± 7	2.8 ± 0.4	13.2			
$B^0 \to D_s^+ \rho^-$	$D_s^+ \to \phi\pi^+$	1190	11 ± 9	1102 ± 36	76 ± 17	12.1			
	$D_s^+ \to \overline{K}^{*0}K^+$	644	3 ± 3	584 ± 27	56 ± 13	3.3	1.3σ	$1.1^{+0.9}_{-0.8} \pm 0.3$	
	$D_s^+ \to K_S^0K^+$	613	4 ± 3	544 ± 26	68 ± 13	8.3		<2.4 (90% C.L.)	
$B^0 \to D_s^{*+} \rho^-$	$D_s^+ \to \phi\pi^+$	194	21 ± 9	175^{+13}_{-12}	0.8 ± 0.2	6.3			
	$D_s^+ \to \overline{K}^{*0}K^+$	101	7 ± 4	93 ± 10	2.3 ± 0.4	1.9	3.7σ	$4.1^{+1.3}_{-1.2} \pm 0.4$	$0.84^{+0.26}_{-0.28} \pm 0.13$
	$D_s^+ \to K_S^0K^+$	91	7 ± 4	80^{+10}_{-9}	3.3 ± 0.9	4.6			
$B^0 \to D_s^- K^+$	$D_s^+ \to \phi\pi^+$	307	53 ± 9	240 ± 17	14 ± 7	22.9			
	$D_s^+ \to \overline{K}^{*0}K^+$	262	22 ± 5	227 ± 16	10 ± 6	8.2	11σ	$2.9 \pm 0.4 \pm 0.2$	
	$D_s^+ \to K_S^0K^+$	148	20 ± 3	125 ± 12	6 ± 5	17.4			
$B^0 \to D_s^{*-} K^+$	$D_s^+ \to \phi\pi^+$	76	28 ± 5	47 ± 8	2.1 ± 0.3	15.2			
	$D_s^+ \to \overline{K}^{*0}K^+$	50	12 ± 3	39 ± 7	0.6 ± 0.1	5.7	7.4σ	$2.4 \pm 0.4 \pm 0.2$	
	$D_s^+ \to K_S^0K^+$	34	11 ± 2	21 ± 5	0.5 ± 0.1	12.0			
$B^0 \to D_s^- K^{*+}$ $K^{*+} \to K_S^0\pi^+$	$D_s^+ \to \phi\pi^+$	95	9 ± 3	83^{+10}_{-9}	5 ± 4	13.8			
	$D_s^+ \to \overline{K}^{*0}K^+$	45	4 ± 1	40 ± 7	1 ± 2	5.4			
	$D_s^+ \to K_S^0K^+$	33	3 ± 1	27^{+6}_{-5}	1 ± 3	10.2			
$K^{*+} \to K^+\pi^0$	$D_s^+ \to \phi\pi^+$	157	8 ± 3	150 ± 13	1 ± 4	9.0	4.6σ	$3.5^{+1.0}_{-0.9} \pm 0.4$	
	$D_s^+ \to \overline{K}^{*0}K^+$	94	3 ± 1	83 ± 10	7 ± 4	3.1			
	$D_s^+ \to K_S^0K^+$	96	3 ± 1	83 ± 10	10 ± 5	7.1			
$B^0 \to D_s^{*-} K^{*+}$ $K^{*+} \to K_S^0\pi^+$	$D_s^+ \to \phi\pi^+$	16	3 ± 2	14 ± 4	0.7 ± 0.4	6.7			
	$D_s^+ \to \overline{K}^{*0}K^+$	8	2 ± 1	7 ± 3	0.3 ± 0.2	2.5			
	$D_s^+ \to K_S^0K^+$	7	1 ± 1	6 ± 3	0.2 ± 0.1	5.2			
$K^{*+} \to K^+\pi^0$	$D_s^+ \to \phi\pi^+$	30	4 ± 2	22 ± 6	0.5 ± 0.2	5.1	3.2σ	$3.2^{+1.4}_{-1.2} \pm 0.4$	$0.92^{+0.37}_{-0.31} \pm 0.07$
	$D_s^+ \to \overline{K}^{*0}K^+$	3	2 ± 1	3 ± 2	0.1 ± 0.1	1.8			
	$D_s^+ \to K_S^0K^+$	11	2 ± 1	9 ± 4	0.2 ± 0.1	4.1			

Uncertainties due to reflection and crossfeed backgrounds include the uncertainties in the branching fractions of the relevant modes, and also account for the contributions of the subdominant modes that are not explicitly included in the ML fit. These contributions dominate the systematic uncertainty for the $B^0 \to D_s^+ \rho^-$ mode, which has a small absolute branching fraction.

As ML estimators may be biased in small samples, we measure the bias using a large ensemble of simulated experiments. In each of these experiments, generated according to the sample composition observed in data, the signal and B-decay background events are fully simulated, and the combinatorial background events are generated from their PDFs. The bias is found to be negligible for the 1- and 2-dimensional ML fits ($B^0 \to D_s^{(*)+}\pi^-$, $B^0 \to D_s^{(*)-}K^+$, $B^0 \to D_s^- K^{*+}$ modes). On the other hand, we find that in the vector-vector modes ($B^0 \to D_s^{*+}\rho^-$ and $B^0 \to D_s^{*-}K^{*+}$ decays), the 3-dimensional ML fits underestimate the true values of the signal branching fraction and the fraction of the longitudinal polarization. We correct for the biases of $\Delta\mathcal{B} = (-0.14 \pm 0.01) \times 10^{-5}$ and $\Delta f_L = (-3.1 \pm 0.3)\%$ ($B^0 \to D_s^{*+}\rho^-$) and $\Delta\mathcal{B} = (-0.34 \pm 0.03) \times 10^{-5}$ and $\Delta f_L = (-1.8 \pm 0.4)\%$ ($B^0 \to D_s^{*-}K^{*+}$). We assign a conservative uncertainty of 50% of the bias to this correction.

For the longitudinal polarization fractions f_L in the vector-vector modes, the systematic errors are dominated by the uncertainties in the shapes of the signal and back-

TABLE III. Relative systematic uncertainties for the branching fractions of $B^0 \to D_s X$ modes (%).

	$B^0 \to D_s^+ \pi^-$	$B^0 \to D_s^- K^+$	$B^0 \to D_s^+ \rho^-$	$B^0 \to D_s^- K^{*+}$
$N_{B\overline{B}}$	1.1	1.1	1.1	1.1
Tracking efficiency	1.6	1.3	1.7	2.0
PID efficiency	1.0	1.0	1.0	1.0
π^0 efficiency	...	...	3.0	3.0
R_L cut efficiency	1.6	1.4	2.8	2.0
MC statistics	0.8	0.7	1.8	1.1
K_S^0 efficiency	0.4	0.3	0.9	0.0
PDF parameters	0.8	0.7	2.8	1.4
ΔE, $m(D_s)$ PDFs	0.6	1.7	3.2	1.7
$\mathcal{B}(D_s^+ \to \phi\pi^+)$	5.7	5.2	10.1	5.7
$\mathcal{B}(D_s^+ \to \overline{K}^{*0} K^+)$	2.9	3.1	1.8	3.1
$\mathcal{B}(D_s^+ \to K_S^0 K^+)$	1.6	1.4	3.7	0.6
Reflection background	2.0	0.7	10.2	0.6
Crossfeed background	0.9	0.5	15.6	2.6
Resonant line shape	1.6	1.7	1.8	4.9
TOTAL	7.8	7.2	22.6	9.9

TABLE IV. Relative systematic uncertainties for the branching fractions of $B^0 \to D_s^* X$ modes (%).

	$B^0 \to D_s^{*+} \pi^-$	$B^0 \to D_s^{*-} K^+$	$B^0 \to D_s^{*+} \rho^-$	$B^0 \to D_s^{*-} K^{*+}$
$N_{B\overline{B}}$	1.1	1.1	1.1	1.1
Tracking efficiency	1.6	1.3	1.7	2.0
PID efficiency	1.0	1.0	1.0	1.0
π^0 efficiency	...	...	3.0	3.0
γ efficiency	1.8	1.8	1.8	1.8
$\mathcal{B}(D_s^{*+} \to D_s^+ \gamma)$	0.7	0.7	0.7	0.7
$\Delta m(D_s^{*+})$	1.0	1.0	1.0	1.0
$\cos\theta_{D_s^{*+}}$	1.0	1.0	1.0	1.0
π^0 veto efficiency	...	...	2.0	2.0
Fit bias	...	...	1.6	5.6
R_L cut efficiency	1.5	1.7	2.3	1.6
MC statistics	0.8	0.8	1.1	1.6
K_S^0 efficiency	0.4	0.0	0.2	0.3
PDF parameters	1.9	2.1	3.0	3.1
ΔE, $m(D_s)$ PDFs	3.0	0.8	0.7	3.4
$\mathcal{B}(D_s^+ \to \phi\pi^+)$	5.4	5.9	5.5	5.0
$\mathcal{B}(D_s^+ \to \overline{K}^{*0} K^+)$	2.7	3.8	3.4	4.1
$\mathcal{B}(D_s^+ \to K_S^0 K^+)$	1.5	1.3	0.9	1.3
Reflection background	3.5	0.0	2.1	0.0
Crossfeed background	1.9	0.4	0.0	1.6
Resonant line shape	0.8	0.4	1.6	0.1
TOTAL	9.0	8.3	9.6	11.3

TABLE V. Absolute systematic uncertainties for the longitudinal polarization fraction (%).

	$B^0 \to D_s^{*+}\rho^-$	$B^0 \to D_s^{*-}K^{*+}$
Fit bias	1.6	0.9
R_L cut efficiency	0.7	0.2
MC statistics	0.6	0.7
K_S^0 efficiency	0.4	0.0
PDF parameters	14.7	7.0
ΔE, $m(D_s)$ PDFs	0.0	0.5
$\mathcal{B}(D_s^+ \to \phi\pi^+)$	0.4	2.0
$\mathcal{B}(D_s^+ \to \overline{K}^{*0}K^+)$	0.7	0.2
$\mathcal{B}(D_s^+ \to K_S^0K^+)$	0.5	0.2
Reflection background	0.5	0.0
Crossfeed background	0.0	0.6
Resonant line shape	0.6	0.1
TOTAL	14.9	7.4

ground PDFs and the fit bias. The systematic uncertainties for each mode are summarized in Tables III, IV, and V.

VI. RESULTS

We estimate the significance of a nonzero signal yield by computing $\mathcal{S} = \sqrt{-2\log(\mathcal{L}_0/\mathcal{L}_{\rm max})}$, where $\mathcal{L}_{\rm max}$ is the maximum likelihood value, and $\mathcal{L}_0$ is the likelihood for a fit in which the signal contribution is set to zero. Including systematic uncertainties and assuming Gaussian-distributed errors, we obtain signal observation significances of 3.7 ($B^0 \to D_s^{*+}\rho^-$), 4.6 ($B^0 \to D_s^-K^{*+}$), and 3.2 ($B^0 \to D_s^{*-}K^{*+}$) standard deviations, providing the first evidence for these decays. We test that $\mathcal{S}$ measures the probability for the background events to fluctuate to the observed number of signal events with a large ensemble of simulated experiments. For each such experiment, we generate a set of pure background events according to the PDFs and sample composition observed in our data set. We then fit each simulated experiment and measure the signal and background yields and, for the vector-vector modes, the polarization fraction f_L. By counting the fraction of such pseudoexperiments in which the signal yields are at least as large as the yield observed in the real data set, we confirm that $\mathcal{S}^2$ follows closely the χ^2 distribution with one degree of freedom.

The branching fraction and polarization results are collected in Table II. Since we do not observe a significant event yield in $B^0 \to D_s^+\rho^-$, we set a 90% confidence-level Bayesian upper limit assuming a constant prior for $\mathcal{B}(B^0 \to D_s^+\rho^-) > 0$.

VII. CONCLUSIONS

We report the following improved measurements of the branching fractions for the rare decays $B^0 \to D_s^{(*)+}\pi^-$ and $B^0 \to D_s^{(*)-}K^+$, and the first measurements of the branching fractions for the decays $B^0 \to D_s^{(*)+}\rho^-$ and $B^0 \to D_s^{(*)-}K^{*+}$, as well as the measurements of the longitudinal polarization fractions f_L in vector-vector final states $B^0 \to D_s^{*+}\rho^-$ and $B^0 \to D_s^{*-}K^{*+}$:

$$\begin{aligned}
\mathcal{B}(B^0 \to D_s^+\pi^-) &= [2.5 \pm 0.4 \pm 0.2] \times 10^{-5},\\
\mathcal{B}(B^0 \to D_s^{*+}\pi^-) &= [2.6^{+0.5}_{-0.4} \pm 0.2] \times 10^{-5},\\
\mathcal{B}(B^0 \to D_s^+\rho^-) &= [1.1^{+0.9}_{-0.8} \pm 0.3] \times 10^{-5},\\
\mathcal{B}(B^0 \to D_s^+\rho^-) &< 2.4 \times 10^{-5}\ (90\%\ \text{C.L.}),\\
\mathcal{B}(B^0 \to D_s^{*+}\rho^-) &= [4.1^{+1.3}_{-1.2} \pm 0.4] \times 10^{-5},\\
f_L(B^0 \to D_s^{*+}\rho^-) &= 0.84^{+0.26}_{-0.28} \pm 0.13,\\
\mathcal{B}(B^0 \to D_s^-K^+) &= [2.9 \pm 0.4 \pm 0.2] \times 10^{-5},\\
\mathcal{B}(B^0 \to D_s^{*-}K^+) &= [2.4 \pm 0.4 \pm 0.2] \times 10^{-5},\\
\mathcal{B}(B^0 \to D_s^-K^{*+}) &= [3.5^{+1.0}_{-0.9} \pm 0.4] \times 10^{-5},\\
\mathcal{B}(B^0 \to D_s^{*-}K^{*+}) &= [3.2^{+1.4}_{-1.2} \pm 0.4] \times 10^{-5},\\
f_L(B^0 \to D_s^{*-}K^{*+}) &= 0.92^{+0.37}_{-0.31} \pm 0.07,
\end{aligned}$$

where the first quoted uncertainty is statistical, and the second is systematic.

The branching fractions for $B^0 \to D_s^{(*)-}K^{(*)+}$ are small compared to the dominant decays $B^0 \to D^{(*)-}\pi^+$ and $B^0 \to D^{(*)-}\rho^+$, implying insignificant contributions from the color-suppressed W-exchange diagrams. The ratios $\mathcal{B}(B^0 \to D_s^-K^+)/\mathcal{B}(B^0 \to D_s^{*-}K^+)$ and $\mathcal{B}(B^0 \to D_s^-K^{*+})/\mathcal{B}(B^0 \to D_s^{*-}K^{*+})$ are consistent with the expectation of unity [12]. The predictions for the branching fractions of $B^0 \to D_s^{(*)+}\pi^-$ and $B^0 \to D_s^{(*)+}\rho^-$ decays are based on the factorization assumption [14] and depend on the estimates of the hadronic form factors. The observed pattern $\mathcal{B}(B^0 \to D_s^+\rho^-) < \mathcal{B}(B^0 \to D_s^+\pi^-) \approx \mathcal{B}(B^0 \to D_s^{*+}\pi^-) < \mathcal{B}(B^0 \to D_s^{*+}\rho^-)$ appears to be most consistent with the form factors computed in [26]. The polarizations of the vector mesons in $B^0 \to D_s^{*+}\rho^-$ and $B^0 \to D_s^{*-}K^{*+}$ are consistent with expectations [12,13].

Assuming the SU(3) relation, Eq. (2), the recent value of $f_{D_s^{(*)}}/f_{D^{(*)}} = 1.24 \pm 0.07$ from an unquenched lattice QCD calculation [9], and the following branching fractions for the CKM-favored decays [20]:

$$\begin{aligned}
\mathcal{B}(B^0 \to D^-\pi^+) &= (2.68 \pm 0.13) \times 10^{-3},\\
\mathcal{B}(B^0 \to D^{*-}\pi^+) &= (2.76 \pm 0.13) \times 10^{-3},\\
\mathcal{B}(B^0 \to D^-\rho^+) &= (7.5 \pm 1.2) \times 10^{-3},\\
\mathcal{B}(B^0 \to D^{*-}\rho^+) &= (6.8 \pm 0.9) \times 10^{-3},
\end{aligned}$$

we determine the ratios of the CKM-suppressed to CKM-favored decay amplitudes in the decays $B^0 \to D^{(*)\pm}\pi^{\mp}$ and $B^0 \to D^{(*)\pm}\rho^{\mp}$:

$$r(D\pi) = [1.78^{+0.14}_{-0.13}(\text{stat}) \pm 0.08(\text{syst}) \pm 0.10(\text{th})]\%,$$
$$r(D^*\pi) = [1.81^{+0.16}_{-0.15}(\text{stat}) \pm 0.09(\text{syst}) \pm 0.10(\text{th})]\%,$$
$$r(D\rho) = [0.71^{+0.29}_{-0.27}(\text{stat}) \pm 0.10(\text{syst}) \pm 0.04(\text{th})]\%,$$
$$r(D^*\rho) = [1.45^{+0.23}_{-0.22}(\text{stat}) \pm 0.12(\text{syst}) \pm 0.08(\text{th})]\%,$$

where the first error is statistical, the second includes experimental systematics, and the last accounts for the uncertainty in the theoretical value of $f_{D_s^{(*)}}/f_{D^{(*)}}$ [9]. These amplitude ratios are below 2%, which implies small CP asymmetries in $B^0 \to D^{(*)\mp}\pi^{\pm}$ and $B^0 \to D^{(*)\mp}\rho^{\pm}$ decays, making it difficult to measure $\sin(2\beta + \gamma)$ precisely in these decays. The results presented here supersede our previously published measurements [15].

ACKNOWLEDGMENTS

We are grateful for the extraordinary contributions of our PEP-II colleagues in achieving the excellent luminosity and machine conditions that have made this work possible. The success of this project also relies critically on the expertise and dedication of the computing organizations that support *BABAR*. The collaborating institutions wish to thank SLAC for its support and the kind hospitality extended to them. This work is supported by the US Department of Energy and National Science Foundation, the Natural Sciences and Engineering Research Council (Canada), the Commissariat à l'Energie Atomique and Institut National de Physique Nucléaire et de Physique des Particules (France), the Bundesministerium für Bildung und Forschung and Deutsche Forschungsgemeinschaft (Germany), the Istituto Nazionale di Fisica Nucleare (Italy), the Foundation for Fundamental Research on Matter (The Netherlands), the Research Council of Norway, the Ministry of Education and Science of the Russian Federation, Ministerio de Educación y Ciencia (Spain), and the Science and Technology Facilities Council (United Kingdom). Individuals have received support from the Marie-Curie IEF program (European Union) and the A. P. Sloan Foundation.

[1] N. Cabibbo, Phys. Rev. Lett. **10**, 531 (1963); M. Kobayashi and T. Maskawa, Prog. Theor. Phys. **49**, 652 (1973).
[2] *CP Violation*, edited by C. Jarlskog, Advanced Series on Directions in High Energy Physics Vol. 3 (World Scientific, Singapore, 1989).
[3] B. Aubert *et al.* (*BABAR* Collaboration), Phys. Rev. Lett. **87**, 091801 (2001); K. Abe *et al.* (Belle Collaboration), Phys. Rev. Lett. **87**, 091802 (2001).
[4] Charge conjugation is implied throughout this paper, unless explicitly stated.
[5] I. Dunietz, Phys. Lett. B **427**, 179 (1998); I. Dunietz and R. G. Sachs, Phys. Rev. D **37**, 3186 (1988); D. A. Suprun, C.-W. Chiang, and J. L. Rosner, Phys. Rev. D **65**, 054025 (2002).
[6] B. Aubert *et al.* (*BABAR* Collaboration), Phys. Rev. Lett. **92**, 251801 (2004); **92**, 251802 (2004).
[7] B. Aubert *et al.* (*BABAR* Collaboration), Phys. Rev. D **73**, 111101 (2006).
[8] D. Becirevic, arXiv:hep-ph/0310072; C. Aubin *et al.*, Phys. Rev. D **70**, 094505 (2004); E. Follana *et al.*, Phys. Rev. Lett. **100**, 062002 (2008).
[9] C. Aubin *et al.*, Phys. Rev. Lett. **95**, 122002 (2005).
[10] K. M. Ecklund *et al.* (CLEO Collaboration), Phys. Rev. Lett. **100**, 161801 (2008).
[11] M. Baak, Ph.D. thesis, Vrije University [Report No. SLAC-R-858, 2007].
[12] S. Mantry, D. Pirjol, and I. W. Stewart, Phys. Rev. D **68**, 114009 (2003).
[13] A. Ali *et al.*, Z. Phys. C **1**, 269 (1979).
[14] D. Choudhury *et al.*, Phys. Rev. D **45**, 217 (1992); C. S. Kim *et al.*, Phys. Rev. D **63**, 094506 (2001).
[15] B. Aubert *et al.* (*BABAR* Collaboration), Phys. Rev. Lett. **90**, 181803 (2003); **98**, 081801 (2007).
[16] PEP-II Conceptual Design Report, SLAC-0418, 1993.
[17] B. Aubert *et al.* (*BABAR* Collaboration), Nucl. Instrum. Methods Phys. Res., Sect. A **479**, 1 (2002).
[18] S. Agostinelli *et al.*, Nucl. Instrum. Methods Phys. Res., Sect. A **506**, 250 (2003).
[19] G. C. Fox and S. Wolfram, Phys. Rev. Lett. **41**, 1581 (1978).
[20] W.-M. Yao *et al.* (Particle Data Group), J. Phys. G **33**, 1 (2006) and 2007 partial update for 2008.
[21] B. Aubert *et al.* (*BABAR* Collaboration), Phys. Rev. Lett. **89**, 281802 (2002); Phys. Rev. D **70**, 032006 (2004).
[22] B. Aubert *et al.* (*BABAR* Collaboration), Phys. Rev. Lett. **100**, 171803 (2008).
[23] J. P. Alexander *et al.* (CLEO Collaboration), Phys. Rev. Lett. **100**, 161804 (2008).
[24] M. J. Oreglia, Ph.D. thesis, Stanford University [Report No. SLAC-236, 1980], Appendix D; J. E. Gaiser, Ph.D. thesis, Stanford University [Report No. SLAC-255, 1982], Appendix F; T. Skwarnicki, Ph.D. thesis, Cracow, INP [Report No. DESY F31-86-02, 1986], Appendix E.
[25] H. Albrecht *et al.* (ARGUS Collaboration), Z. Phys. C **48**, 543 (1990).
[26] M. Wirbel, B. Stech, and M. Bauer, Z. Phys. C **29**, 637 (1985); **34**, 103 (1987).